ACS APPLIED MATERIALS & INTERFACES

Research Article

www.acsami.org

# Nonspherical Double Emulsions with Multiple Distinct Cores Enveloped by Ultrathin Shells

Sang Seok Lee,[†] Alireza Abbaspourrad,[‡] and Shin-Hyun Kim*[,†]

[†]Department of Chemical and Biomolecular Engineering and KINC, KAIST, Daejeon 305-701, Korea

[‡]School of Engineering and Applied Sciences, Harvard University, Cambridge, Massachusetts, United States

Supporting Information

**ABSTRACT:** Microfluidics has provided means to control emulsification, enabling the production of highly monodisperse double-emulsion drops; they have served as useful templates for production of microcapsules. To provide new opportunities for double-emulsion templates, here, we report a new design of capillary microfluidic devices that create nonspherical double-emulsion drops with multiple distinct cores covered by ultrathin middle layer. To accomplish this, we parallelize capillary channels, each of which has a biphasic flow in a form of core−sheath stream; this is achieved by preferential wetting of oil to the hydrophobic wall. These core−sheath streams from the parallelized channels are concurrently emulsified into continuous phase, making paired double-emulsion drops composed of multiple cores and very thin middle shell. This microfluidic approach provides high degree of controllability and flexibility on size, shape, number, and composition of double-emulsion drops. Such double-emulsion drops are useful as templates to produce microcapsules with multicompartments which can encapsulate and deliver multiple distinct components, while avoiding their cross-contamination. In addition, nonspherical envelope exerts strong capillary force, leading to preferential coalescence between innermost drops; this is potentially useful for nanoliter-scale reactions and encapsulations of the reaction products.

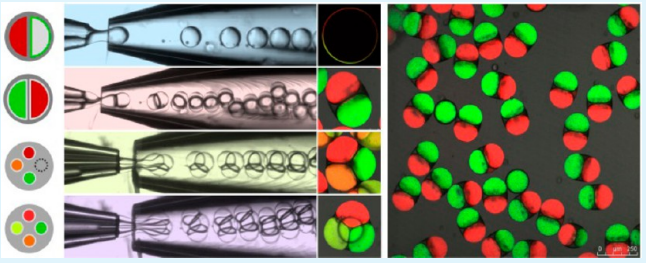

**KEYWORDS:** *microfluidics, double emulsion, capsules, coalescence, capillary*

## INTRODUCTION

Microfluidic technologies have been employed to make monodisperse emulsion drops, which can serve as microtest tubes for biological analysis[1,2] or templates for fabrication of functional microparticles.[3−5] In particular, microfluidic devices made of either poly(dimethylsiloxane) (PDMS) or glass capillaries have enabled production of double-emulsion drops with a high degree of controllability and flexibility on size, shape, and number of inner drops, providing very useful templates to make microcapsules owing to their core−shell geometry.[6−11] Even higher flexibility can be achieved by incorporation of multiple distinct innermost drops into outer drops;[12−16] this facilitates simultaneous encapsulation of multiple components into their own compartments, while avoiding their cross-contaminations. Although previous methods enable the incorporation of two or three different innermost drops to outer drops in a controlled fashion, a relatively large volume of the middle phase—the typical volume ratio of the middle to innermost droplets is larger than 0.5—is required to encapsulate the innermost drops safely, which frequently results in low emulsion stability and thick capsule membranes; these yield rupture of core−shell structure and low payload in the interior of capsules, respectively. Moreover, injection of the middle phase through a single channel produces a homogeneous middle layer that encapsulates all distinct innermost drops. By contrast, encapsulation of each innermost drop with its own shell can provide a higher flexibility for controlled release of the encapsulants; release sequence and rate of encapsultants can be independently adjusted by controlling each shell composition. Although double-emulsion drops with Janus middle layer are produced in PDMS device, they are composed of one innermost drop engulfed by a thick middle layer.[17] Therefore, microfluidic emulsification techniques with a higher controllability in the size, number, and composition of both innermost and outer drops remain an important challenge to create functional microcapsules for simultaneous storage of multiple distinct components and their controlled release.

In this article, we report a new design of capillary microfluidic device which creates monodisperse double-emulsion drops with multiple distinct innermost drops covered by their own ultrathin middle layers. Using theta ($\theta$)-shaped or multibore capillaries, we create core−sheath biphasic flow in each parallel capillary channel, which is concurrently emulsified along with neighboring fluids into continuous phase; this results in the formation of paired double-emulsion drops comprising multiple distinct innermost drops with an ultrathin shells. The number of the innermost drops is determined by the number of the

Received: November 21, 2013
Accepted: January 1, 2014
Published: January 1, 2014

  

core−sheath flows; in addition, the relative size of the innermost drops is precisely controlled by relative flow rates. Moreover, injection of middle phases through separate channels enables us to encase innermost drops with distinct middle layers. These double-emulsion drops with enhanced complexity can be permanently captured by consolidation of the middle phase, thereby providing solid microcapsules. By contrast, to use the drops as microreactors, the drops can be incubated without solidification, which can lead to a selective coalescence and mixing between the innermost drops while the double-emulsion membrane remains intact.

## RESULTS AND DISCUSSION

### 2.1. Double-Emulsion Drops with Dumbbell Shape.

To make double-emulsion drops containing two different innermost drops, we use a microfluidic device whose injection capillary has theta ($\theta$) shape in its cross-section, as illustrated schematically in Figure 1a. To simultaneously inject two immiscible fluids through each hemispherical channel of theta-shaped capillary, two small tapered capillaries are inserted. An image of the capillary device is shown in Figure S1a of the Supporting Information. We inject 10 wt % aqueous solution of polyvinyl alcohol (PVA) through one of the small tapered capillaries to form innermost drops. As middle phases, three types of oils are employed: Monomer of ethoxylated trimethylolpropane triacrylate (ETPTA), kerosene solution containing 8% surfactant of polyglycerol polyricinoleate (PGPR) 90, and chloroform solution containing 20 wt % poly(lactic acid) (PLA); one of these oil phases is injected through the other small tapered capillary. We use 10 wt % aqueous solution of PVA as a continuous phase and inject this through the interstices between the injection and the square capillaries. As two immiscible fluids, water and oil phases, are injected through each channel of the theta-shaped injection capillary, the water phase forms a train of pluglike drops without contacting the capillary wall, whereas the oil phase becomes continuous phase of the drops by flowing along the wall due to hydrophobic nature of the capillary surface.[18] The core−sheath flows are formed in both channels of the theta-shaped capillary and then, they are concurrently emulsified into the continuous phase at the tip of the injection capillary in a dripping mode, where high flow rate at the narrow orifice of collection capillary obviates the formation of a jet.

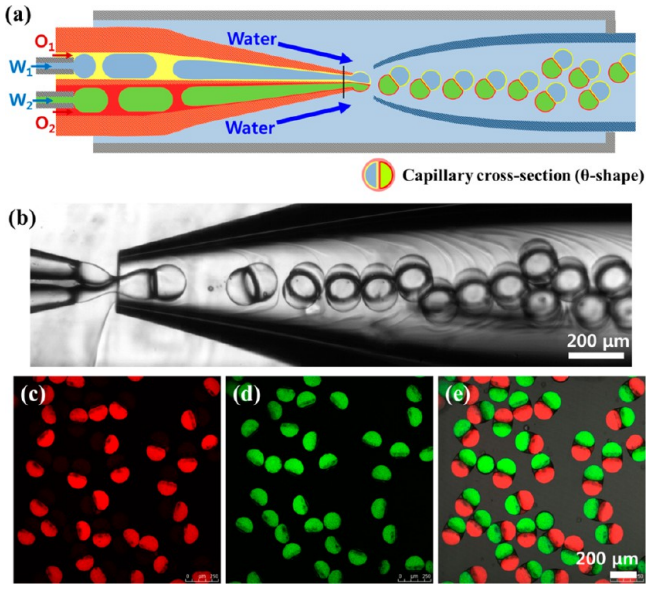


**Figure 1.** (a) Schematic illustration of the microfluidic device for preparation of double-emulsion drops with two distinct innermost drops covered by two different ultrathin shells. (b) Optical microscope images showing generation of symmetric dumbbell-shaped double-emulsion drops, where flow rates of two inner ($Q_{i1}$ and $Q_{i2}$), two middle ($Q_{m1}$ and $Q_{m2}$), and continuous ($Q_c$) phases are maintained at values of 300, 200, and 6000 $\mu$L/h, respectively. (c−e) Confocal microscope images of dumbbell-shaped double-emulsion drops encapsulating two distinct materials, red dye and green dye, in their separate bulbs.

During the emulsification, three different types of drops are alternatively produced because of discontinuous flow of plug-like drops. When the plug-like drops from both channels are coemulsified, dumbbell-shaped double-emulsion drops, containing two distinct innermost drops covered by a very thin middle layer, are generated as shown in Figure 1b and Movie S1 in the Supporting Information. The detail of the drop formation is shown in a series of still shot images in Figure S1b in the Supporting Information. When one channel has the pluglike drops and the other channel has oil flow, spherical double-emulsion drops containing one innermost drop covered by a thick middle layer are generated as shown in Figure S2a, c in the Supporting Information. For only oil flows at both channels, single oil drops are generated. Although all three different types of drops are produced, the dumbbell-shaped drops are easily separated by exploiting their density difference from others; average density of the dumbbells is almost identical to the density of the innermost water phase due to very small volume of the middle phase: Typical volume ratio of the oil to innermost aqueous phase is 0.05−0.08, which results in shells with a thickness of 0.8−1.4 $\mu$m for drops with diameter of 100 $\mu$m.[18] By comparison, conventional methods typically provide the volume ratio larger than 0.5.[16,19] For example, monodisperse dumbbells, with a middle phase of kerosene, can be separated from the mixture, as shown in Figure 1c−e, where one aqueous bulb has red dye of sulforhodamine B and the other bulb has green dye of fluorescein; single oil drops and double-emulsion drops with thick shell rise upward because of the much lower density of kerosene than that of water, whereas double-emulsion drops with very thin shells are concentrated on the bottom of collection liquid, an aqueous mixture of 2 wt % PVA and 40 mM NaCl. This collection liquid is carefully selected to have slightly lower density than that of the innermost water, 10 wt % aqueous solution of PVA, but the same osmolarity, thereby avoiding water flux across the liquid membrane. The double-emulsion drops remain intact longer than one day and any leakage of dye is not observed. Volumetric proportion of the dumbbells among all three types of drops is determined by flow rates of the inner ($Q_i$) and middle ($Q_m$) phases. For the same $Q_i$ and $Q_m$ in both channels, the maximum proportion is estimated as $Q_i/(Q_i + Q_m)$ which can be achieved when the plug-like drops formations at both channels are synchronized; in this case, there is no production of double-emulsion drops with a thick shell. When the formations are anti-synchronized, the minimum proportion of the dumbbells is produced as $(Q_i - Q_m)/(Q_i + Q_m)$, where production of double-emulsion drops with a thick shell is maximized. To achieve the high proportion, we maintain $Q_i/Q_m$ as high as 1.3−2, which ensures approximately 40−50% of the dumbbells over all drops.


dx.doi.org/10.1021/am405283j | ACS Appl. Mater. Interfaces 2014, 6, 1294−1300

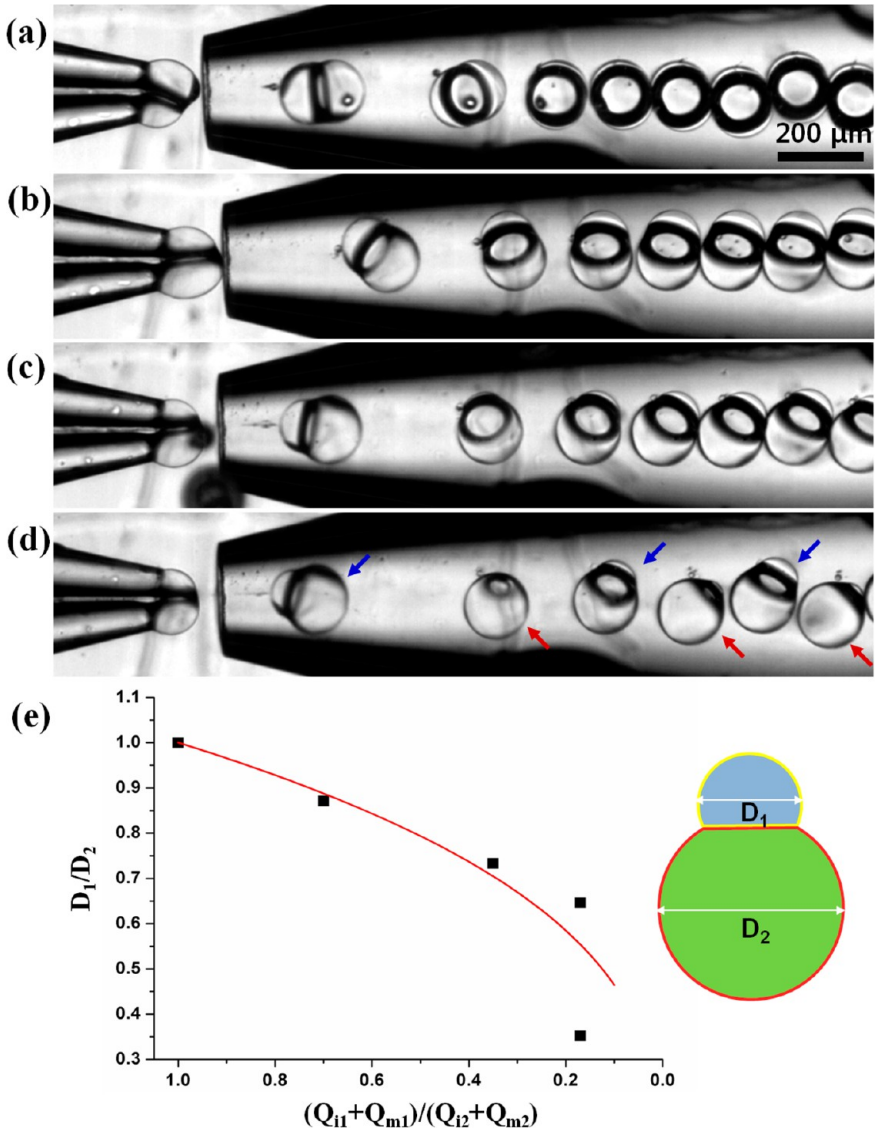


**Figure 2.** (a–d) Optical microscope images showing generation of symmetric or asymmetric dumbbell-shaped double-emulsion drops at four different sets of flow rates of $Q_{i1}$, $Q_{m1}$, $Q_{i2}$, and $Q_{m2}$ of (a) 300, 200, 300, and 200 $\mu$L/h; (b) 200, 150, 300, and 200 $\mu$L/h; (c) 100, 75, 300, and 200 $\mu$L/h; and (d) 50, 35, 300, and 200 $\mu$L/h, where $Q_c$ is maintained at 6000 $\mu$L/h; (d) shows alternative generation of two different asymmetric dumbbells as denoted by blue and red arrows. (e) Relative diameter $(D_1/D_2)$ of bulbs of the dumbbell-shaped double-emulsion drops as a function of relative flow rate. The curve is drawn by eq 1

**2.2. Control of Dumbbell Symmetry.** Relative bulb size of the dumbbells can be adjusted by their flow rate ratio. Because the core–sheath flows from both channels are coemulsified in the same frequency, relative volume of bulbs from channel 1 to bulbs from channel 2 is estimated as $(Q_{i1} + Q_{m1})/(Q_{i2} + Q_{m2})$. For example, symmetric dumbbells, with middle phase of ETPTA, are generated with the same flow rates for both channels, as shown in Figure 2a. When we decrease $(Q_{i1} + Q_{m1})/(Q_{i2} + Q_{m2})$ from 1 to 0.7 and 0.35, monodisperse asymmetric dumbbells are generated, as shown in images b and c in Figure 2, respectively. For a further decrease to 0.17, two different asymmetric dumbbells are alternatively generated as shown in Figure 2d, where dumbbells with large relative diameter of bulb 1 to bulb 2, $D_1/D_2$, are denoted by blue arrows and dumbbells with small relative diameter are denoted by red arrows. We attribute the production of two different asymmetric dumbbells to retraction of interface. At such a low flow rate, the interface retracts toward to the tip immediately after its breakup due to insufficient supply of fluids. At the next moment of drop formation, very small volume of the retracted fluids is coemulsified with neighboring fluids due to its adhesion to the neighbor without accumulation of the fluids, yielding a very small bulb. Then, the interface advances because of the slow but continuous supply of fluids, thereby being concurrently dragged along with neighboring fluids by continuous phase at the next moment of breakup, forming relatively large bulb; in this case, the interface passes beyond the position of interface breakup. Generation and flow of all symmetric and asymmetric dumbbells are shown in Movie S2 in the Supporting Information; the last part of the movie clearly shows the formation of two different asymmetric dumbbells. We summarize variation in the relative diameter, $D_1/D_2$, as a function of relative flow rate in Figure 2e, where two squares at 0.17 correspond to two different asymmetric dumbbells, and the curve is

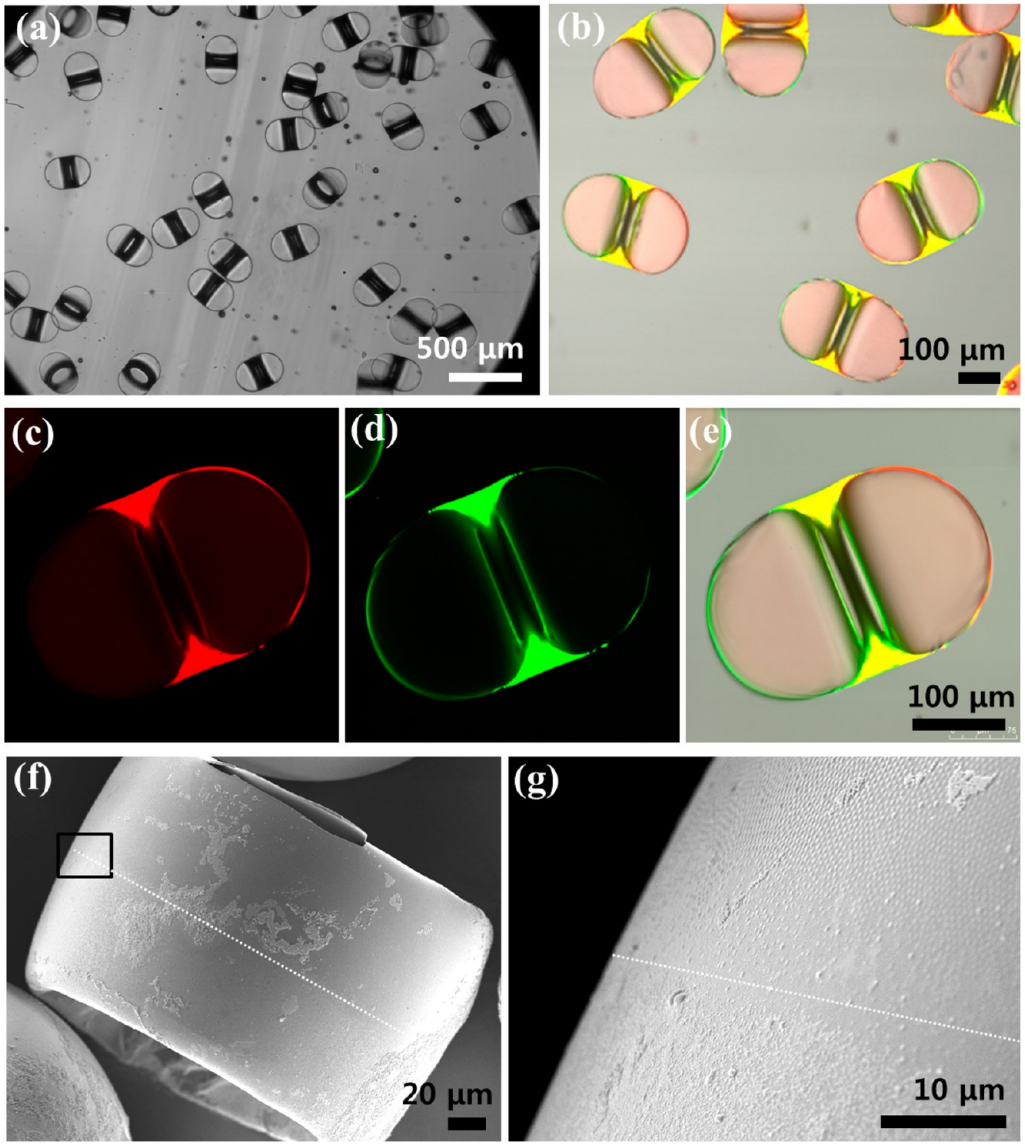


**Figure 3.** (a–e) Optical and confocal microscope images of dumbbell-shaped microcapsules composed of two distinct membranes: One is doped with green dye and the other is doped with red dye. (f, g) Scanning electron microscope (SEM) images of dried microcapsules composed of two distinct membranes: One contains 500 nm silica particles on its surface and the other contains 200 nm silica particles. A boundary between two membranes is denoted by a dotted line.

$$\frac{D_1}{D_2} = \left(\frac{Q_{i1} + Q_{m1}}{Q_{i2} + Q_{m2}}\right)^{1/3} \quad (1)$$

which gives rough estimation of the relative diameter. Examples of monodisperse symmetric and asymmetric dumbbells, with a middle phase of kerosene, are shown in Figure S3 of the Supporting Information.

**2.3. Distinctive Shells in Dumbbell.** Middle phases of dumbbells are injected through separate channels, thereby enabling encapsulation of two distinct innermost cores with their own specific shells, as schematically illustrated in Figure 1a. We demonstrate this using two middle phases: ETPTA containing red dye of Nile red and 500 nm silica particles (middle phase 1) and ETPTA containing green dyes of Coumarin 540 and 200 nm silica particles (middle phase 2); both silica particles and dyes are employed to observe boundary between distinct domains of shell. We inject these two middle phases through separate channels of the theta-shaped capillary and produce the double-emulsion drops. To photopolymerize the monomers and form dumbbell-shaped capsules, we expose the drops to UV light in the collection bath for 10 s. Although the dumbbell drops are unstable against coalescence of innermost drops, polymerization permanently solidifies the middle phase, creating stable microcapsules, as shown in Figure 3a; size distribution of the dumbbells is shown in Figure S4 in the Supporting Information. We can confirm the existence of two different middle membranes with a confocal microscope, as shown in Figure 3b–e; in spite of autofluorescence of ETPTA, two separate green and red membranes are clearly shown in the images. Intensity profile of each fluorescent signal across the capsule is shown in Figure S5a, b in the Supporting Information. In addition, we can observe the boundary between the two different membranes using scanning electron microscope (SEM). Silica particles, dispersed in each ETPTA middle phase, adsorb at water-ETPTA interfaces before photopolymerization,[20,21] enabling the observation of the boundary.


dx.doi.org/10.1021/am405283j | ACS Appl. Mater. Interfaces 2014, 6, 1294–1300

During preparation of SEM sample, the capsule membranes are fully deflated inward due to evaporation of water from the cores as shown in Figure 3f. We can clearly observe the boundary which locates on the middle body of the capsules as denoted by the dotted line in Figure 3f, g and Figure S5c in the Supporting Information, where the surface above the line is composed of hexagonal array of 500 nm silica particles and the surface below the line is composed of 200 nm silica particles.

**2.4. Selective Coalescence Between Innermost Drops.** Nonspherical envelope of middle layer exerts a strong capillary force on the innermost drops, which leads to slow but continuous drainage of the middle phase from the thinnest parts of the layer. Therefore, the dumbbells cannot maintain their structure for a long time without appropriate surfactants or solidification of middle phase; appropriate surfactants might maintain some distance between two interfaces at molecular scale and finally stop the drainage, resulting in stable nonspherical double-emulsion drops. For example, the dumbbells with a middle phase of kerosene with 8% PGPR 90 survive more than one day, whereas the dumbbells with a middle phase composed of either unpolymerized ETPTA or chloroform solution containing 20 wt % PLA, exhibit coalescence between the innermost drops within a few minutes after generation, resulting in spherical double-emulsion drops with a single core covered by a thin shell, as schematically illustrated in Figure 4a.

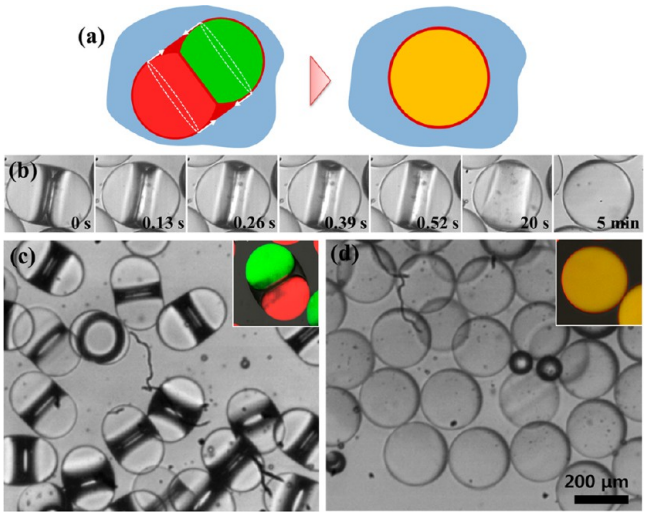


**Figure 4.** (a) Schematic illustration of the coalescence of two innermost drops. Arrows denote direction of capillary force. (b) Series of optical microscope images showing coalescence of two innermost drops, taken at the times denoted in the images. (c, d) Optical microscope images of monodisperse double-emulsion drops (c) before and (d) after coalescence of two innermost drops. Confocal microscope images in insets show mixing of red and green dye upon coalescence.

We attribute this preferential coalescence between innermost drops to stronger lubrication resistance in the oil film between the outer envelope and the overhanging surfaces of the innermost droplets in comparison with the resistance in the oil film between two innermost droplets. The outer envelope and the overhanging surfaces of the innermost droplets have almost same curvatures, thereby leading to strong lubrication resistance and relatively slow drainage of the middle phase;[18,22] this is also reason why double-emulsion drops with ultrathin shell are more stable than normal ones. By contrast, the oil film between two innermost drops is sandwiched by interfaces with opposite curvatures, leading to relatively weaker lubrication resistance and therefore faster drainage from the film. Therefore, two interfaces of innermost droplets approach to each other relatively fast, therefore finally making preferential coalescence between the innermost drops without appropriate surfactants. In conventional double-emulsion drops with multicores and thick shells, the innermost drops frequently coalesce with continuous phase, thereby rupturing, instead of coalescence between the innermost drops due to weak lubrication resistance. Preferential coalescence of two innermost drops in double-emulsion drops, with an ultrathin middle phase of chloroform solution containing 20 wt % PLA, is shown in a series of optical microscope images of Figure 4b. As soon as the drops are coalesced, double-emulsion drop recovers the spherical shape in 1 s. However, it takes a few minutes to distribute the oil uniformly through whole middle layer. The dumbbell-shaped double-emulsion drops before the coalescence and spherical double-emulsion drops after the coalescence are shown in images c and d in Figure 4, respectively; confocal microscope images in the insets show mixing of green and red dyes upon coalescence. This selective coalescence without rupture is useful for nanoliter-scale reaction[23−28] and subsequent encapsulation of the product. For example, drugs which form crystals and precipitates as they are produced through reaction can be simply encapsulated with this approach; this is difficult to achieve with the conventional microfluidic technique because of the clogging of channels.

**2.5. Distinctive Shells in Sphere.** Operating the same device without injecting one of innermost aqueous phases, we can produce double-emulsion drops with single core covered by two different middle phases, as schematically illustrated in Figure 5a. To make microcapsules composed of spherical membrane with two domains, we use the same set of two different ETPTA monomers used for the dumbbell capsules. We set the flow rates of $Q_{i2}$, $Q_{m1}$, and $Q_{m2}$ as 300, 30, and 200 $\mu$L/h, respectively, to produce double-emulsion drops as shown in Figure 5b and Movie S3 in the Supporting Information. We fabricate monodisperse microcapsules with solidified membrane by photopolymerizing ETPTA as shown in Figure 5c; confocal microscope image shows two hemispherical membranes with different colors as illustrated in Figure 5d. In addition, we can observe the boundary between two membranes, one composed of 500 nm silica particles and the other composed of 200 nm silica particles, on their surface and the cross-section as shown in SEM images e and f in Figure 5, respectively; diffusion of colloids within the membrane makes the boundary less clear in the cross-section.

**2.6. Triangular and Tetrahedron Double-Emulsion Drops.** To incorporate multiple distinct innermost drops, we use a four-bore capillary as the injection capillary in the device as shown in Figure S6a in the Supporting Information. When we operate the device with three core−sheath flows from three bores and no flow from one bore, we can produce monodisperse double-emulsion drops with three distinct cores which are covered by a very thin shell as shown in Figure 6a. Resultant triangular double-emulsion drops are shown in Figure 6d−f, where the three innermost drops contain red dye, green dye, and a mixture of red and green dyes, respectively. Although other types of single- or double-emulsion drops with thick shell are also alternatively produced, separation of the triangles can be easily achieved by exploiting the density difference in the same fashion to the case of

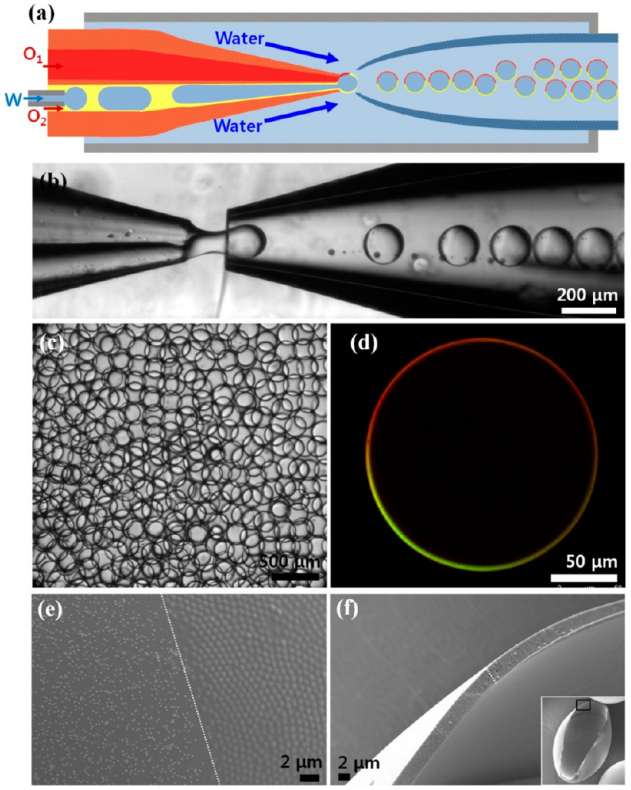


**Figure 5.** (a) Schematic illustration of the microfluidic device for preparation of double-emulsion drops containing single innermost drop covered by an ultrathin shell with two distinct domains. (b) Optical microscope images showing generation of double-emulsion drops, where $Q_{i2}$, $Q_{m1}$, $Q_{m2}$, and $Q_c$ are maintained at values of 300, 30, 200, and 6000 $\mu$L/h, respectively. (c, d) Optical and confocal microscope images of microcapsules composed of two distinct membranes: One is doped with green dye and the other is doped with red dye. (e, f) SEM images of surface and cross-section of a dried microcapsule composed of two distinct membranes: One contains 500 nm silica particles on its surface and the other contains 200 nm silica particles. A boundary between two membranes is denoted by dotted line.

dumbbell-shaped double-emulsion drops. By employing oil flow at the remaining one channel, we can produce the triangular double-emulsion drops with relatively thick shell as shown in Figure 6b, where dark flow from one channel is oil, which makes the double-emulsion drops more relaxed against the compressive capillary force. When we fully operate the device with four core–sheath flows, four distinct innermost drops are incorporated into one double-emulsion drops, as shown in Figure 6c; each core–sheath flow from separate channels maintains the core–shell structure during emulsification because each sheath flow prevents direct contact between the core drops. A breakup of four parallel streams occurs at the same time, making planar-diamond-shaped drops. However, they quickly transform to tetrahedron shape to minimize their interfacial energy, as shown in Figure S6b in the Supporting Information; the relative volume of oil shell to innermost drops in these double-emulsion drops with ultrathin shell is approximately 10-fold smaller than that of previous double-emulsion drops with densely packed cores.[19]

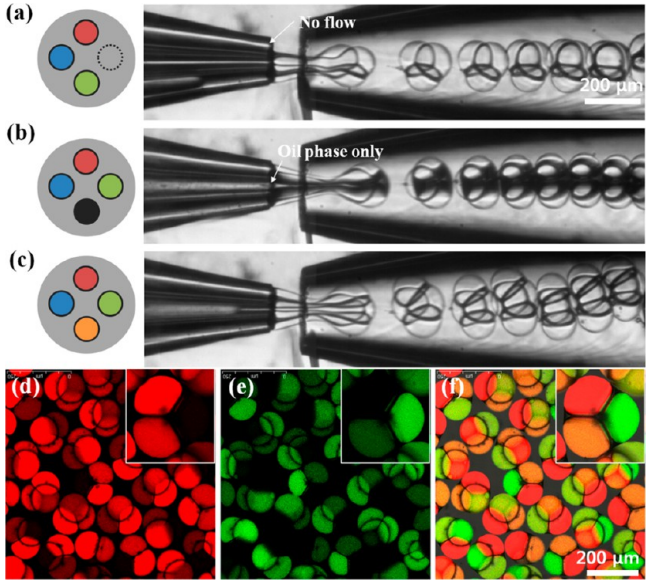


**Figure 6.** (a–c) Sets of schematic illustration of the cross sections of injection capillary and optical microscope image showing generation of double-emulsion drops with three or four distinct innermost drops. (d–f) Confocal microscope images of triangular double-emulsion drops with three distinct innermost drops encapsulating red dye, green dye, and both dyes.

## CONCLUSIONS

We produce monodisperse double-emulsion drops containing multiple distinct cores covered with an ultrathin middle layer through coemulsification of parallel biphasic flows. To accomplish this, we create the core–sheath flows in each of parallelized injection capillaries by using preferential wetting of a fluid with higher affinity to wall, and then concurrently emulsify them into the continuous phase in a dripping mode. The number of distinct innermost drops is determined by the number of the core–sheath flows and relative size of the innermost drops can be controlled by flow rates. Moreover, each innermost drop can be encapsulated by its own middle phase, thereby creating distinct domains of membranes. These multicored double-emulsion drops with an ultrathin middle layer can serve as promising templates to make microcapsules which can deliver multiple distinct components such as drugs, cosmetics, detergents, and nutrients, while avoiding their cross-contamination; photo-cross-linkable and biocompatible prepolymers can be used to produce the capsules for in vivo applications.[29] In addition, sequential release of the materials can also be potentially achieved by employing different membrane materials encapsulating different innermost drops. Moreover, the nonspherical envelope of the drops, caused by a very small volume of middle phase, enables the selective coalescence between the innermost drops without rupture, which will provide a new opportunity to use the double-emulsion drops as not just microreactors but also microcompartments for encapsulation of the products of the reaction.

## MATERIALS AND METHODS

**Materials.** As innermost and continuous phases of double-emulsion drops, 10 wt % aqueous solution of PVA ($M_w$ 13 000–23 000, Sigma-Aldrich) is used; water-soluble dye molecules of sulforhodamine B (Sigma-Aldrich) or fluorescein (Sigma-Aldrich) are sometimes dissolved in the innermost phase as model encapsulants. As middle oil phases, three types of oils are employed:


dx.doi.org/10.1021/am405283j | ACS Appl. Mater. Interfaces 2014, 6, 1294–1300

ETPTA (Sigma-Adrich) containing 0.2 wt % photoinitiator of 2-hydroxy-2-methylpropiophenone (Sigma-Aldrich), kerosene solution containing 8% surfactant of PGPR 90, and chloroform solution containing 20 wt % PLA ($M_w$ 15 000, Polyscience, Inc.); oil-soluble dye molecules of Nile red (9-diethylamino-5-benzo[$\alpha$]phenoxazinone, Sigma-Aldrich) or Coumarin 540 (3-(2-benzothiazolyl)-7-(diethylamino)-2H-1-benzopyran-2-one, Exiton) are dissolved to visualize distinct domains of shell. Silica particles used in some experiments are synthesized by the two-phase method.[30]

**Preparation of Microfluidic Device and Its Operation.** To make capillary microfluidic devices, we tapered and assembled two cylindrical capillaries in a square capillary. For injection channels, either the theta-shaped capillary (World precision instruments, Inc., TST150−6) or four-bore capillary (VitroCom, Inc., FB1562) is tapered by micropipette puller (P97, Sutter Instrument) and treated with n-octadecyltrimethoxy silane (Sigma-Aldrich) to make the capillary wall hydrophobic. For collection channels, round cylindrical capillary (World precision instruments, Inc., 1B150−6) is tapered and treated with 2-[methoxy(polyethyleneoxy)propyl] trimethoxy silane (Gelest, Inc.) to make the capillary wall hydrophilic. These two cylindrical capillaries are inserted into the opposite ends of a square capillary (AIT) and coaxially aligned. In addition, one or two small tapered capillaries are inserted into each channel of the injection capillary to simultaneously inject two immiscible fluids. The flow rates of innermost, middle, and continuous phases are independently controlled by syringe pumps (Harvard apparatus) and drop formation is observed by high speed camera (Phantom V9). For polymerization of ETPTA, spot UV system (Omnicure S1000) is used.

## ■ ASSOCIATED CONTENT

### Ⓢ Supporting Information

Optical microscope images showing drop generation and confocal microscope images of the resultant double-emulsion drops and capsules are included. In addition, Movies S1−3 show the generation of drops in microfluidic devices. This material is available free of charge via the Internet at http://pubs.acs.org.

## ■ AUTHOR INFORMATION

### Corresponding Author

*E-mail: kim.sh@kaist.ac.kr. Tel: +82 42 350 3911. Fax: +82 42 350 3910.

### Notes

*Notes.* The authors declare no competing financial interest.

## ■ ACKNOWLEDGMENTS

This work was supported by the KAIST Startup Fund (Project G04120012), HRHRP (Project N10130008) and International Collaboration grant (Sunjin-2010-002) from the Korean Ministry of Knowledge Economy. Part of this research was carried out at Harvard University, kindly hosted by Prof. D. A. Weitz. We dedicate this article to late Professor Seung-Man Yang for his lifelong contribution to colloid and interface science.

## ■ REFERENCES

(1) Agresti, J. J.; Antipov, E.; Abate, A. R.; Ahn, K.; Rowat, A. C.; Baret, J. C.; Marquez, M.; Klibanov, A. M.; Griffiths, A. D.; Weitz, D. A. *Proc. Natl. Acad. Sci. U.S.A.* **2010**, *107*, 4004.
(2) Griffiths, A. D.; Tawfik, D. S. *Trends Biotechnol.* **2006**, *24*, 395.
(3) Dendukuri, D.; Doyle, P. S. *Adv. Mater.* **2009**, *21*, 4071.
(4) Il Park, J.; Saffari, A.; Kumar, S.; Gunther, A.; Kumacheva, E. *Annu. Rev. Mater. Res.* **2010**, *40*, 415.
(5) Kim, S. H.; Lee, S. Y.; Yang, S. M. *Angew. Chem., Int. Ed.* **2010**, *49*, 2535.
(6) Okushima, S.; Nisisako, T.; Torii, T.; Higuchi, T. *Langmuir* **2004**, *20*, 9905.
(7) Utada, A. S.; Lorenceau, E.; Link, D. R.; Kaplan, P. D.; Stone, H. A.; Weitz, D. A. *Science* **2005**, *308*, 537.
(8) Kim, S. H.; Jeon, S. J.; Yang, S. M. *J. Am. Chem. Soc.* **2008**, *130*, 6040.
(9) Lee, D.; Weitz, D. A. *Small* **2009**, *5*, 1932.
(10) Lee, M. H.; Hribar, K. C.; Brugarolas, T.; Kamat, N. P.; Burdick, J. A.; Lee, D. *Adv. Funct. Mater.* **2012**, *22*, 131.
(11) Deng, N.-N.; Wang, W.; Ju, X.-J.; Xie, R.; Weitz, D. A.; Chu, L.-Y. *Lab Chip* **2013**, *13*, 4047.
(12) Kim, S. H.; Shim, J. W.; Yang, S. M. *Angew. Chem., Int. Ed.* **2011**, *50*, 1171.
(13) Shum, H. C.; Zhao, Y. J.; Kim, S. H.; Weitz, D. A. *Angew. Chem., Int. Ed.* **2011**, *50*, 1648.
(14) Sun, B. J.; Shum, H. C.; Holtze, C.; Weitz, D. A. *ACS Appl. Mater. Interfaces* **2010**, *2*, 3411.
(15) Zhao, Y.; Xie, Z.; Gu, H.; Jin, L.; Zhao, X.; Wang, B.; Gu, Z. *NPG Asia Mater.* **2012**, *4*, e25.
(16) Wang, W.; Xie, R.; Ju, X.-J.; Luo, T.; Liu, L.; Weitz, D. A.; Chu, L.-Y. *Lab Chip* **2011**, *11*, 1587.
(17) Seiffert, S.; Romanowsky, M. B.; Weitz, D. A. *Langmuir* **2010**, *26*, 14842.
(18) Kim, S. H.; Kim, J. W.; Cho, J. C.; Weitz, D. A. *Lab Chip* **2011**, *11*, 3162.
(19) Kim, S. H.; Hwang, H.; Lim, C. H.; Shim, J. W.; Yang, S. M. *Adv. Funct. Mater.* **2011**, *21*, 1608.
(20) Binks, B. P.; Lumsdon, S. O. *Langmuir* **2000**, *16*, 8622.
(21) Kim, S. H.; Abbaspourrad, A.; Weitz, D. A. *J. Am. Chem. Soc.* **2011**, *133*, 5516.
(22) Kim, P. G.; Stone, H. A. *Europhys. Lett.* **2008**, *83*, 54001.
(23) Song, H.; Chen, D. L.; Ismagilov, R. F. *Angew. Chem., Int. Ed.* **2006**, *45*, 7336.
(24) Hung, L.-H.; Choi, K. M.; Tseng, W.-Y.; Tan, Y.-C.; Sheab, K. J.; Lee, A. P. *Lab Chip* **2006**, *6*, 174.
(25) Chen, H.; Zhao, Y.; Li, J.; Guo, M.; Wan, J.; Weitz, D. A.; Stone, H. A. *Lab Chip* **2011**, *11*, 2312.
(26) Kim, Y. H.; Zhang, L.; Yu, T.; Jin, M.; Qin, D.; Xia, Y. *Small* **2013**, *9*, 3462.
(27) Bannock, J. H.; Krishnadasan, S. H.; Nightingale, A. M.; Yau, C. P.; Khaw, K.; Burkitt, D.; Halls, J. J. M.; Heeney, M.; de Mello, J. C. *Adv. Funct. Mater.* **2013**, *23*, 2123.
(28) Koziej, D.; Floryan, C.; Sperling, R. A.; Ehrlicher, A. J.; Issadore, D.; Westervlet, R.; Weitz, D. A. *Nanoscale* **2013**, *5*, 5468.
(29) Hwang, D. K.; Oakey, J.; Toner, M.; Arthur, J. A.; Anseth, K. S.; Lee, S.; Zeiger, A.; Van Vliet, K. J.; Doyle, P. S. *J. Am. Chem. Soc.* **2009**, *131*, 4499.
(30) Hartlen, K. D.; Athanasopoulos, A. P. T.; Kitaev, V. *Langmuir* **2008**, *24*, 1714.